Applied Energy 226 (2018) 935–946

Contents lists available at ScienceDirect

Applied Energy

journal homepage: www.elsevier.com/locate/apenergy

System-level energy consumption modeling and optimization for cellulosic biofuel production

Yuntian Ge, Lin Li*

Department of Mechanical and Industrial Engineering, University of Illinois at Chicago, Chicago, IL 60607, USA

HIGHLIGHTS

- A system-level energy model for cellulosic biofuel production is proposed.
- The relationships between energy and production parameters are studied.
- A numerical case is conducted to identify the major energy drivers.
- The impacts of decision variables on energy consumption are analyzed.
- The optimization results in 21.09% reduction in total energy consumption.

ARTICLE INFO

Keywords:
Cellulosic biofuel
Biofuel production
System modeling
Energy analysis
Energy consumption optimization

ABSTRACT

As a promising alternative to fossil fuels, cellulosic biofuel has obtained considerable interest due to its potential for mitigating global climate change and enhancing energy security. However, the widespread adoption of cellulosic biofuel is taking place in a slower pace than expected. One major challenge is that the cellulosic biofuel production is still highly energy-intensive. In fact, the energy contained in cellulosic biofuel is less than the energy required for its production. To address this issue, in this paper, an analytical system-level energy model is proposed to characterize the fundamental relationships between total energy consumption and biofuel production parameters in cellulosic biofuel production systems. Furthermore, an optimization strategy based on Particle Swarm Optimization (PSO) is adopted to minimize the energy consumption of cellulosic biofuel production while maintaining the desired biofuel yield. A baseline case is implemented for analyzing energy consumption, and the results show that pretreatment consumes most energy among all processes and the water/biomass ratio is the most significant energy driver. In addition, the optimal solution results in a 21.09% reduction in the total energy consumption compared to the baseline case.

1. Introduction

In 2017, the global greenhouse gas (GHG) emissions have reached an all-time high [1], meanwhile, 62% of these emissions are from burning fossil fuels [2]. The extensive use of fossil fuels has led to serious issues like climate change, environmental pollution, human health, and energy supply challenges associated with the irreversible depletion of fossil fuels [3]. Hence, many countries are turning their attentions to new, clean, and sustainable energy sources, e.g., solar energy, wind energy, biofuel, etc.

Biofuel, as one of the most popular renewable energy sources, is expected to play a crucial role in future global energy infrastructure. Currently, biofuel is the only viable and widely available source of renewable transportation energy [4,5]. Based on different biomass feedstocks, biofuels can be divided into several categories such as sugarcane biofuel, cellulosic biofuel, algae biofuel, etc. Among various types of biofuels, cellulosic biofuel is considered to be the most promising alternative to help mitigate the global climate change [6] due to its wide available feedstock resources and low lifecycle GHG emissions. It is reported that using cellulosic ethanol can achieve up to 90% GHG saving compared to petroleum fuels [7].

Despite the aforementioned advantages, cellulosic biomass needs to go through several energy intensive production processes before these benefits can be realized. A typical cellulosic biofuel production system usually includes size reduction, pretreatment, enzymatic hydrolysis, and fermentation process. During the size reduction process, the raw cellulosic biomass is cut and grinded into small particles for further biochemical conversions. Next, in the pretreatment process, the

* Corresponding author.
E-mail address: linli@uic.edu (L. Li).

https://doi.org/10.1016/j.apenergy.2018.06.020
Received 26 February 2018; Received in revised form 6 May 2018; Accepted 2 June 2018
Available online 15 June 2018
0306-2619/ © 2018 Elsevier Ltd. All rights reserved.

Nomenclature

Bold face

S	solution vector to the optimization problem
X	particle position vector
V	particle velocity vector

Upper case

A	pre-exponential factor (1/s)
A^p	pretreatment reactor surface area (m^2)
A^h	hydrolysis reactor surface area (m^2)
A^f	fermentation reactor surface area (m^2)
C_{acid}	active acid concentration (w/w%)
C_k	Kick's constant
C_{pw}	specific heat capacity of water (KJ/mol/K)
C_{pb}	specific heat capacity of biomass (KJ/mol/K)
C_{pa}	specific heat capacity of acid (KJ/mol/K)
D_e	diffusion coefficient (m^2/s)
E_a	activation energy (kJ/mol)
H_L	latent heat of water vaporization (KJ/kg)
K_g	inhibition constant of xylose (g/L)
K_{xl}	inhibition constants of xylose (g/L)
L_1	particle size before reduction (mm)
L_2	particle size after reduction (mm)
M_g	molecular weight of glucan (g/mol)
M_{gl}	molecular weight of glucose (g/mol)
M_x	molecular weight of xylan (g/mol)
M_{xl}	molecular weight of xylose (g/mol)
M_{xo}	molecular weight of xylose oligomer (g/mol)
N_p	number of particles in the swarm
$P_{i,g}$	threshold ethanol concentration of glucose (g/mol)
$P_{i,x}$	threshold ethanol concentration of xylose (g/mol)
$P_{m,g}$	maximum ethanol concentration of glucose (g/mol)
$P_{m,x}$	maximum ethanol concentration of xylose (g/mol)
$Q_{heatloss}$	energy to balance heat loss (KJ)
$Q_{heating}$	energy for heating (KJ)
$Q_{reaction}$	reaction energy (KJ)
$Q_{recovery}$	recovered energy (KJ)
$Q_{size\ reduction}$	energy required in size reduction process (KJ)
R	gas constant
R_1	inner radius of the reactor (m)
R_2	outer radius of the reactor(m)
T_p	pretreatment temperature (°C)
T_h	enzymatic hydrolysis temperature (°C)
T_f	fermentation temperature (°C)

Lower case

a	ratio of the liquid volume and solid spheres volume
c_1	learning factor
c_2	learning factor
c_e	concentration of ethanol (kg/L)
c_g	concentration of glucose (kg/L)
c_{xl}	concentration of xylose (kg/L)
c_{xo}	concentration of xylose oligomer (kg/L)
c_z	concentration of recombinant (kg/L)
h_{out}	convection coefficient ($W/m^2/°C$)
m_a	mass of diluted acid (kg)
m_b	mass of biomass (kg)
m_w	mass of water (kg)
k_{pipe}	thermal conductivity of the reactor (W/m/°C)
t_p	pretreatment time (min)
t_f	fermentation time (hour)
t_h	enzymatic hydrolysis time (hour)
k	reaction rate (1/s)
$q_{emax,g}$	maximum specific ethanol production rate by glucose (g/L)
$q_{emax,x}$	maximum specific ethanol production rate by xylose (g/L)
q_n	reaction constant
$q_{smax,g}$	maximum specific glucose utilization rate (g/L)
$q_{smax,x}$	maximum specific xylose utilization rate (g/L)
p_g	mass of glucan in feedstock (kg)
p_x	mass of xylan in feedstock (kg)

Greek

ρ_w	density of water (kg/m^3)

recalcitrant structure of the lignocellulosic material is weakened and most hemicellulose carbohydrates (i.e., xylan, galactan, arabinan, mannan) are converted into soluble sugars. In the enzymatic hydrolysis process, cellulose is catalyzed by enzymes to release shorter chains and ultimately soluble sugars. Finally, these sugars are converted into ethanol in the fermentation process.

In the current literature, numerous studies have been carried out on different aspects of biofuel production. For biomass processing, the effects of various factors on biofuel production are investigated including biomass type [8–11], biomass size [12–14], biomass particle properties [15,16], etc. For biofuel conversion processes, research efforts have been devoted to the improvement of the pretreatment process [17–19], the development of cellulase enzyme [20,21], and genetically modification of fermentation microbe [22,23], etc. Furthermore, lifecycle analysis [24,25] and economic performance evaluations of biofuel production [26,27] have also been conducted.

The aforementioned studies provide considerable knowledge and innovative technological advancements in biofuel production. However, the challenge regarding the high energy demand in producing cellulosic biofuel still exists. It is reported that 1.27 MJ of energy are required to produce 1 MJ ethanol, where 63% is consumed in the production processes [28]. Currently, most studies on the energy analysis of biofuel production adopt the Life Cycle Assessment (LCA) approach to estimate the energy usage and analyze the environmental impacts [7,24,25,29,30]. However, LCA models are typically linear steady-state models [31], and thus cannot be used to reduce the production energy usage by identifying the optimum system production parameters (e.g., pretreatment temperature, feedstock particle size, fermentation time, etc.). Therefore, more detailed energy modeling and analyses that consider the relationships between these production parameters and energy consumption are emerging, which can be classified into two main categories: simulation-based and analytical studies.

The majority of simulation-based studies use Aspen software to simulate biofuel conversion in single or multiple processes [32–38]. The advantage of simulation-based methods is that they can capture system performance in the quite complex biofuel production systems. However, like LCA models, they are not able to reveal the fundamental mathematical relationships between system parameters and performance measures. Furthermore, the development and execution of simulation models to obtain statistically useful results may be prohibitively expensive and slow, which makes it quite difficult to find optimal solutions.

Compared to simulation-based studies, much less research uses analytical modeling methods due to the difficulties in establishing mathematical relationships between biofuel production parameters and energy consumption. Only a few papers that use analytical modeling

methods to study the energy consumption in cellulosic biofuel production are reported in the literature, and they focus on single process rather than whole production system [39,40]. Nevertheless, optimizing the energy consumption in one process will not necessarily lead to the system's energy reduction because the processes within cellulosic biofuel production systems are highly interrelated. For example, producing coarser particles in the size reduction process usually requires less energy, which however, might eventually result in a higher total energy consumption since coarser particles require more energy to be converted to biofuel. Furthermore, exclusively optimizing the energy consumption of different processes may cause biofuel production yield loss. Therefore, it is necessary to consider the interrelations between each process and analyze the energy consumption of multiple processes systematically.

In this paper, an analytical system-level energy model for the cellulosic biofuel production system is proposed and established by considering the interrelationships between each process. In addition, the energy consumption is optimized under the constraint of biofuel yield and solved using Particle Swarm Optimization (PSO) algorithm. To the best knowledge of the authors, this work is one of the first analytical methods that characterize the fundamental relationships between the total energy consumption and production parameters in cellulosic biofuel production systems. The establishment of these relationships provides a powerful tool to theoretically predict, evaluate and optimize the energy consumption in cellulosic biofuel production, which will offer valuable guidance in system design and operation. Additionally, the presented optimization strategy enables manufacturers to determine the best production parameters and achieve significant energy savings without compromising biofuel yield. The research outcomes in this paper will help realize energy-efficient biofuel production and enhance the sustainability of cellulosic biofuel.

The rest of this paper is organized as follows. In Section 2, a brief description of the four major processes in the biofuel production system is presented. The analytical model for the energy consumption and ethanol yield is proposed in Section 3. In Section 4, a comprehensive energy analysis is conducted, and the sensitivity analysis is performed by adjusting the baseline parameters. In Section 5, the optimization model is formulated and solved using PSO approach, and the results from optimal solution is compared with the baseline case. Finally, the conclusions and future research directions are discussed in Section 6.

2. Process description

The proposed energy model is based on the cellulosic biofuel production system shown in Fig. 1, which consists of four major processes: size reduction, pretreatment, enzymatic hydrolysis, and fermentation. Note that in this paper corn-stover is used as the biomass feedstock. The solid composition of corn-stover is shown in Table 1.

The biomass size reduction process usually involves grinding or cutting cellulosic feedstock into small pieces. The minced feedstock is screened by sieves with certain sizes. In this process, the biomass' contacting surface area increases greatly so that it can be hydrolyzed into soluble sugar at a fast rate. The main energy intensive activity at this stage comes from the size reduction machines' electricity consumption.

In the pretreatment process, it is assumed that the steam-assisted dilute-acid pretreatment method is adopted [42]. The cellulosic material is mixed with water and broken down under high-temperature (~158 °C) and high-pressure (5 atm) reaction conditions. In the reaction, the crystallinity degree of cellulose is reduced, and the cellulose becomes more amorphous, which is the most suitable form for enzymatic attack. Most of the hemicellulose contained in the feedstock is converted into soluble pentoses (i.e., xylose) that can be utilized as substrates for fermentation. A small fraction of glucan degrades to glucose, while the majority of the glucan remains as solid residues. In this process, energy is mainly consumed by heating the feedstock-water mixture and maintaining the reaction temperature. The heat in the water/steam can be partially recovered while cooling.

In the hydrolysis process, the cellulose chains are broken down to produce glucose for fermentation. Enzymatic hydrolysis is current the most recognized technique for bioethanol hydrolysis because no degradation products of glucose are formed, although the process is rather slow [43]. After the hydrolysis process, most of the cellulosic content (hemicellulose and cellulose) is converted into fermentable sugars. Energy is consumed to cool down the hydrolysis reactor since this reaction is exothermic.

In the fermentation process, all soluble sugars (mainly xylose and glucose) are assumed to be simultaneously fermented into ethanol using recombinant *Zymomonas mobilis* strain *ZM4* (*pZB5*) (*Z. mobilis ZM4* (*pZB5*)) [44]. Meanwhile, energy is supplied to maintain the reaction temperature.

3. Energy consumption modeling

In this section, the mathematical model for the energy consumption is developed. This model is based on the most prevailingly adopted cellulosic biofuel production method, which consists of four main processes, i.e., feedstock size reduction, dilute-acid pretreatment, enzymatic hydrolysis and fermentation of cellulosic feedstock. The proposed model considers five common energy components: energy for feedstock size reduction, heating energy, reaction energy, energy loss, and energy recovery, hence, it can also be adopted for other cellulosic production methods (e.g. Alkaline pretreatment-based cellulosic biofuel production).

3.1. Energy modeling of biomass size reduction process

Generally, energy required in the grinding process can be described by three empirical equations, namely, Rittinger's law, Kick's law, and Bond's law. According to [45], Rittinger's law and Bond's law are often used for smaller particles (< 1 cm), while Kick's law can be used to model the energy consumption of grinding particles larger than 1 cm, which is within the size range of raw biomass feedstock particles. Therefore, in this paper, the Kick's law is adopted to calculate the energy consumption in the size reduction process.

Based on Kick's law [46], it is assumed that the energy required to reduce a material in size is directly proportional to the size reduction

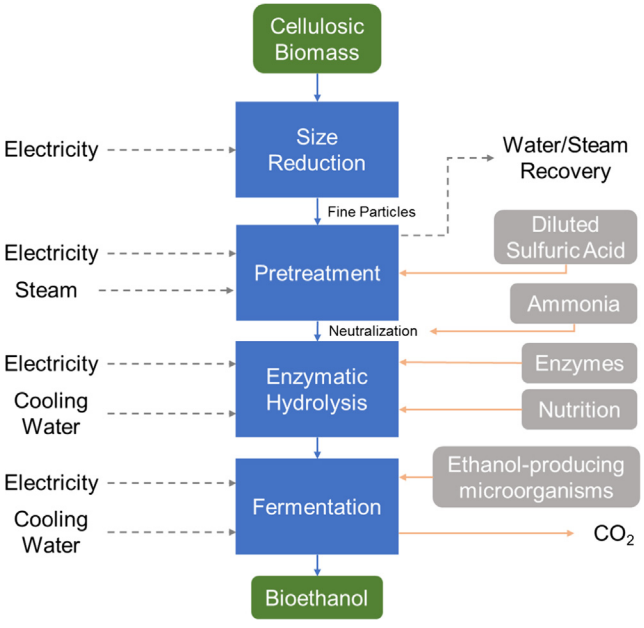

Fig. 1. Block diagram of biofuel production from cellulosic biomass.

Table 1
Solid composition of corn-stover [41].

Component	Dry weight percentage
Glucan	39.1%
Xylan	23.1%
Lignin	16.3%
Galactan	1.8%
Arabinan	3.4%
Mannan	0.3%
Acetyl	2.7%
Structural inorganics	4.8%
Protein	4.5%
Ash	4%

ratio dL/L:

$$\frac{dQ_{\text{size reduction}}}{dL} = C_k \cdot L^{-1}. \quad (1)$$

Performing integration for both side of the equal sign, we have:

$$Q_{\text{size reduction}} = C_k \cdot \ln\left(\frac{L_1}{L_2}\right) \quad (2)$$

where $Q_{size\ reduction}$ is the energy required in this process; C_k is the Kick's constant; L_1 is the particle size before reduction; and L_2 is the particle size after reduction. Particle size is defined as the screen size that the particles can pass through regardless of the particles' shape.

Kick's constant is an experimental constant which depends on the biomass type and grinding machines' properties. In [47], the researchers measured the energy consumption of grinding switchgrass, wheat straw, and corn-stover, where the data of corn-stover is used in this paper to calculate C_k. In [47], the corn-stover used is 150 mm, and it consumes 0.02 KWh when grinded into 25.4 mm at 500 rpm rotor speed and 5 kg/min feeding rate, thus the Kick's constant can be calculated as:

$$C_k = Q_{\text{size reduction}}/\ln(L_1/L_2) = 72(\text{KJ/kg})/\ln(150/25.4) = 40.55.$$

In this work, the corn-stover and grinding machine properties are assumed to be the same as [47]. Hence the Kick's constant C_k of 40.55 is used for the following energy calculations.

3.2. Energy modeling of biofuel chemical conversion processes

In this section, the energy modeling of the three biochemical processes, i.e., pretreatment, enzymatic hydrolysis, and fermentation is presented. Energy in these processes is mainly supplied to heat the reactants and maintain desired reaction temperature. Moreover, in the cooling stages, energy is also partially recovered.

In Fig. 2, the reaction temperature profile during the pretreatment, enzymatic hydrolysis, and fermentation processes is illustrated. The timeline is slotted into 8 stages according to the temperature changes. In the heating stage (i.e., stage H), biomass is mixed with water at room temperature (25 °C), and the mixture is heated up to attain the desired reaction temperature of T_p (> 155 °C). Energy is supplied to maintain this temperature in stage M_1 (usually 5–10 min [48]), during which the oligomers are formed. Then, the heat is released in stage C_1 to cool the contents down to 130 °C. The reactor is kept at 130 °C for about 25 min in stage M_2 to allow the conversion of oligomers to monomers [41]. In stage C_2, the energy continues to be released and the products are cooled down to T_h. Stage M_3 represents the enzymatic hydrolysis process with a residence time of t_h ($t_h \approx 84$ h), during which energy is supplied to maintain the temperature of T_h to ensure the efficiency of the cellulase enzyme. After enzymatic hydrolysis, the saccharified slurry is cooled to T_f for fermentation. Energy is supplied for t_f ($t_f \approx$ 36 h) fermentation to ensure the ethanol yield from the strain of *Z. mobilis*.

3.2.1. Heating energy

The heating energy considered in this model only includes the energy used for heating the biomass, water, and sulfuric acid mixture in pretreatment process. This is because the water input in enzymatic hydrolysis and fermentation are usually not heated to help cool down the reactions. The generic equation of the heating energy is:

$$Q_{heating} = m_w \int_{25}^{T_p} C_{p_w}\, dT + m_b \int_{25}^{T_p} C_{p_b}\, dT + m_a C_{p_a}(T_p - 25) \quad (3)$$

where m_w, m_b and m_a are the mass of water, biomass, and diluted acid, respectively; C_{pw} and C_{pb} are the specific heat capacity of water and biomass, respectively; C_{pa} is the average specific heat capacity of diluted sulfuric acid; and T_p represents the pretreatment temperature.

To calculate the energy required for heating the water from 25 °C to T_p, it is determined that at a pressure of 557 kPa (5.5 atm), water boils at 155 °C. The latent heat of water vaporization (H_L) at 155 °C is adopted. It is assumed 5% of the water evaporates at this temperature, which further results in 95% of water being heated from 155 °C to T_p. According to [49], we can formulate the water and steam heat capacity expressions as:

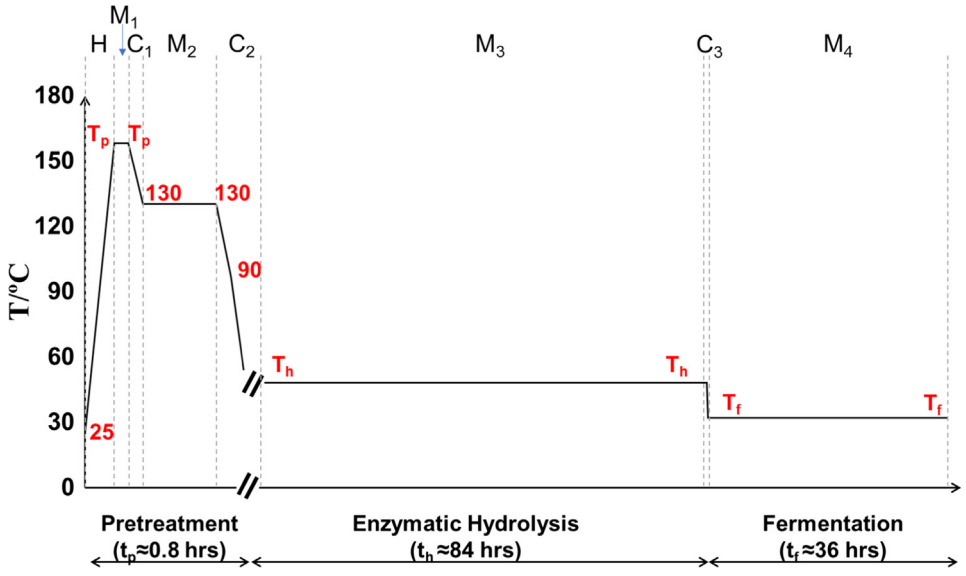

Fig. 2. Reaction temperature profile during pretreatment, enzymatic hydrolysis and fermentation process.

$$C_{p_w} = 0.00001T^2 - 0.0013T + 4.2085 \quad (3\text{-}1)$$

$$C_{p_s} = 0.0000008T^2 + 0.0002T + 1.8572. \quad (3\text{-}2)$$

In addition, we obtain the specific heat capacity of biomass from [39] as:

$$C_{p_b} = 0.00004T^2 - 0.0015T + 0.9325 \quad (3\text{-}3)$$

Consequently, the expression of heating energy is:

$$\begin{aligned} Q_{\text{heating}} = {} & m_w \int_{25}^{155} (0.00001T^2 - 0.0013T + 4.2085)dT + 0.05 m_w H_L \\ & + 0.95 m_w \int_{155}^{T_p} (0.00001T^2 - 0.0013T + 4.2085)dT \\ & + 0.05 m_w \int_{155}^{T_p} (0.0000008T^2 + 0.0002T + 1.8572)dT \\ & + m_b \int_{25}^{T_p} (0.00004T^2 - 0.0015T + 0.9325)dT + m_a \overline{C_{p_a}} (T_p - 25). \end{aligned} \quad (4)$$

3.2.2. Energy loss

Since the reaction temperatures during all the stages (as shown in Fig. 2) are higher than the room temperature (i.e., 25 °C), heat escapes from reactors to the ambient via conduction and convection. In this study, the reactors are assumed to be of a cylindrical nature [41] and as a result, the amount of heat lost during the all processes is formulated as the heat loss of a pipe:

$$Q_{lost} = UA\Delta T \cdot t \quad (5)$$

where A is the surface area of reactor; ΔT represents the temperature difference between the inner side of the reactor and the room temperature; and t is the duration time. In addition, the overall heat transfer coefficient, U, is defined as:

$$U = 1/[(R_2 \ln(R_2/R_1)/k_{pipe}) + 1/h_{out}] \quad (5\text{-}1)$$

where R_1 and R_2 represent the inner and outer radius of the reactor, respectively; k_{pipe} is the thermal conductivity of the reactor; and h_{out} is the convection coefficient at the outside surface.

Since the heating stage residence time is quite short, the temperature rising of the reactor is assumed to be linear. Therefore, the total energy required to offset energy loss and maintain the reaction temperature is:

$$\begin{aligned} Q_{\text{heatloss}} = {} & U^p A^p \int_0^{t_H} t \cdot \left(\frac{T_p - 25}{t_H}\right) dt + \left(\sum_1^2 U^p A^p \Delta T^{M_i}\right) \cdot t_{M_i} + U^h A^h \Delta T^{M_3} \cdot t_h \\ & + U^f A^f \Delta T^{M_4} \cdot t_f \end{aligned} \quad (6)$$

where the superscript/subscript p, h, and f represent the pretreatment, hydrolysis, and fermentation processes, respectively; t_H is the residence time of the heating stage; and M_i (i = 1, 2, 3, 4) represents the stages M_1 to M_4.

3.2.3. Reaction energy

The reaction energy model established in this work is based on the net energy balance for a closed system: the change in the internal energy is equal to the amount of heat supplied to the system, minus the amount of work done by the system on its surroundings. Since all the reactions are taken place in isochoric reactors, the work done by the system is zero. Therefore, the energy absorbed/released due to the reactions is equal to the change of internal energy, which is measured by the internal energy variations between the input materials and output materials in each process. Consequently, the mass of the products in each process needs to be calculated.

3.2.3.1. Chemical reactions of cellulosic biofuel production. Table 2 lists nine major chemical reactions of cellulosic biofuel production. Arabinan, mannan, and galactan are assumed to have the same reactions and conversion pathways as xylan. Heat of Formation (HoF) represents the energy required/released for 1 kg reactant converting to product. The positive values mean that the reaction is endothermic while negative values indicate exothermic reactions.

Catalyzed by diluted-acid, the xylan is converted to xylose and xylose oligomer, which finally is converted to xylose [27]:

$$\begin{aligned} \frac{dp_x}{dt} = -(k_{xo} + k_{xl}) p_x \cdot C_{acid} \quad & \frac{dc_{xo}}{dt} = k_{xo} \cdot \left(\frac{p_x}{M_x}\right)\left(\frac{M_x}{M_{xo}}\right) \cdot C_{acid} \cdot \frac{1}{(m_w/\rho_w)} \\ -k_{x2} \cdot c_{xo} \cdot C_{acid} \quad & \frac{dc_{xl}}{dt} = k_{xl} \cdot \left(\frac{p_x}{M_x}\right)\left(\frac{M_x}{M_{xl}}\right) \cdot C_{acid} \cdot \frac{1}{(m_w/\rho_w)} \\ + k_{x2} \cdot c_{xo} \cdot \left(\frac{M_{xo}}{M_{xl}}\right) \cdot C_{acid} \quad & t \in [0, t_{M_1}] \end{aligned} \quad (7)$$

where p_x, c_{xo}, and c_{xl} represent xylan mass fraction in biomass, xylose-oligomers concentration and xylose concentration, respectively; k_{xo} and k_{xl} are the reaction rates of the conversion from xylan to xylose-oligomers and xylan to xylose, respectively. The reaction rates are assumed to have an Arrhenius dependence [50] on temperature:

$$k = A \cdot e^{-E_a/RT}. \quad (7\text{-}1)$$

The acid concentration C_{acid} is represented by the concentration of acid which has infiltrated feedstock particle. The diffusion into a spherical particle is described by the following partial differential equation:

$$\frac{\partial C}{\partial t} = D_e \left(\frac{\partial^2 C}{\partial r^2} + \frac{2}{r}\frac{\partial C}{\partial r}\right). \quad (7\text{-}2)$$

The analytical solution of this problem is given by Crank [51]:

$$C_{acid}(t) = c_0 \cdot [1 - f(t)] f(t) = 1 - \sum_{n=1}^{\infty} \left(\frac{6a(1+a)}{9 + 9a + q_n^2 a}\right) \exp\left(-\frac{q_n^2 D_e t}{(d/2)^2}\right) \quad (7\text{-}3)$$

where $C_{acid}(t)$ denotes the active acid concentration at time t; and $a = 3 \times (m_w/\rho_w)/[4\pi(L_2/2)^3]$ is the ratio of the liquid volume and solid spheres volume; q_n is a reaction constant; and D_e is the diffusion coefficient.

Table 2
Reactions considered in cellulosic biofuel production.

Process	Reaction	Reactant	Heats of Formation (KJ/kg)[a]
Pretreatment	#1: $(Xylan)_n + n\ H_2O \rightarrow n$ Xylose	Xylan	248.8
	#2: $(Xylan)_n + m\ H_2O \rightarrow m$ Xylose Oligomer	Xylan	1903.2
	#3: $(Glucan)_n + n\ H_2O \rightarrow n$ Glucose	Glucan	279.1
	#4: $(Arabinan)_n + n\ H_2O \rightarrow n$ Arabinose	Arabinan	2102.2
	#5: $(Mannan)_n + n\ H_2O \rightarrow$ Mannose	Mannan	2941.5
	#6: $(Galactan)_n + n\ H_2O \rightarrow$ nGalactose	Galactan	2941.5
Enzymatic Hydrolysis	#7: $(Glucan)_n + n\ H_2O \rightarrow n$ Glucose	Glucan	−1463.1
Fermentation	#8: Glucose → 2 Ethanol + 2 CO_2	Glucose	−1836.9
	#9: 3 Xylose → 5 Ethanol + 5 CO_2	Xylose	−1610.3

[a] Calculated based on the data in the Appendix of [41]. Original data is in the unit of cal/mol.

Table 3
Baseline case decision variables.

Decision variables	Values
Feedstock particle diameter: L_2	6.67 mm (4 mesh)
Water loading (per kg feedstock): m_w	2.2 kg
Diluted acid loading: C_{acid}	1.0% w/w
Pretreatment temperature: T_p	158 °C
Pretreatment time: t_p	5 min
Enzymatic hydrolysis temperature: T_h	48 °C
Enzymatic hydrolysis time: t_h	84 hrs
Fermentation temperature: T_f	32 °C
Fermentation time: t_f	36 hrs

In pretreatment, a fraction of glucan is converted into glucose [27]:

$$\frac{dp_g}{dt} = -k_g \cdot p_g \cdot C_{acid},\ \frac{dc_g}{dt} = k_g \cdot \left(\frac{p_g}{M_g}\right)\left(\frac{M_g}{M_{gl}}\right) \cdot C_{acid} \cdot \frac{1}{(m_w/\rho_w)} \quad t \in [0,\ t_{M_1}] \tag{8}$$

where p_g and c_g represent glucan mass fraction in biomass and glucose concentration, respectively.

In the enzymatic hydrolysis process, a substrate inhibition model is adopted to simulate the glucose formation [52]:

$$\frac{dp_g}{dt} = -\frac{k_h \cdot E_b \cdot p_g}{1 + (c_g/K_g) + (c_{xl}/K_{xl})} \frac{dc_g}{dt} = 1.111 \times \frac{k_h \cdot E_b \cdot p_g \cdot (1/(m_w/\rho_w))}{1 + (c_g/K_g) + (c_{xl}/K_{xl})} \quad t \in [0,\ t_h] \tag{9}$$

where E_b is the enzyme loading; K_g and K_{xl} represent the substrate inhibition coefficient of glucose and xylose, respectively.

In the fermentation process, the xylose and glucose generated from pretreatment and enzymatic hydrolysis are finally converted into ethanol. We simplified the model developed in [53], which based on substrate inhibition and product inhibition, and implement it to calculate the ethanol yield.

$$\begin{aligned}\frac{dc_{xl}}{dt} &= -(1-\alpha) \cdot \frac{q_{\mathrm{smax},x}}{m_w} \cdot \left(1 - \frac{c_e - P_{i,x}}{P_{m,x} - P_{i,x}}\right)\left(\frac{K_{i,x}}{K_{i,x} + c_{xl}}\right) \cdot c_Z \frac{dc_g}{dt} \\ &= -\alpha \cdot \frac{q_{\mathrm{smax},g}}{m_w} \cdot \left(1 - \frac{c_e - P_{i,g}}{P_{m,g} - P_{i,g}}\right)\left(\frac{K_{i,g}}{K_{i,g} + c_g}\right) \cdot c_Z \frac{dc_e}{dt} \\ &= -\left(\frac{q_{\mathrm{emax},x}}{q_{\mathrm{smax},x}} \cdot \frac{dc_{xl}}{dt} + \frac{q_{\mathrm{emax},g}}{q_{\mathrm{smax},g}} \cdot \frac{dc_g}{dt}\right) \quad t \in [0,\ t_f]\end{aligned} \tag{10}$$

where c_e is the concentration of ethanol; c_z is the concentration of ethanol production microbial; q_{smax} is the maximum substrate uptake rate; q_{emax} is the maximum ethanol production rate; P_i is the production inhibition coefficient; P_m is the maximum production inhibition coefficient; and K_i is the substrate inhibition coefficient.

3.2.3.2. Reaction heat modeling. The total reaction energy is calculated by the sum of internal energy changes in all processes. The internal energy change is determined by the conversion rate of the reactant multiply with the heat of formation of corresponding reactions:

$$Q_{\mathrm{reaction}} = \Delta Q_{i,p} + \Delta Q_{i,h} + \Delta Q_{i,f} = \sum_1^9 CR_i \cdot HoF_i = \sum_1^9 \left(\frac{R_i^0 - R_i^E}{R_i^0}\right) \cdot HoF_i \tag{11}$$

where R_i^0 and R_i^E are the mass of the reactant at the beginning and end of the 9 reactions from Table 2, respectively; and HoF_i represents the heat of formation of the corresponding reaction.

3.2.4. Energy recovery

In this model. We consider the energy that potentially could be recovered in Stages C_1 and C_2 (Fig. 1) by calculating the enthalpy changes of the water and biomass at each stage:

Table 4
Energy related parameters.

Parameter	Value
C_k	40.55[a]
H_L	2257 KJ/kg [49]
R_1	1.3 m [41]
R_2	1.315 [41]
k_{pipe}	13.8 W/m/°C [39]
h_{out}	45 W/m^2/°C[a]
A^p	47.78 m^2 [41]
A^h	250 m^2 [41]
A^f	200 m^2 [41]
R	8.314[b]

[a] Calculated in Section 3.1.
[b] Obtained from common knowledge.

$$\begin{aligned}Q_{\mathrm{Recovery}} = \sum_{C_1,C_2} m_{b,remain} \int_{T_1}^{T_2} (0.00004T^2 - 0.0015T + 0.9325)dT \\ + m_w \int_{T_1}^{T_2} (0.00001T^2 - 0.0013T + 4.2085)dT.\end{aligned} \tag{12}$$

In summary, the total energy required to produce ethanol from size reduction process to the end of fermentation can be expressed as a linear combination of all energy components:

$$Q_{total} = Q_{\text{size reduction}} + Q_{\text{heating}} + Q_{\text{heatloss}} + Q_{\text{reaction}} - Q_{\text{recovery}}. \tag{13}$$

4. Energy analysis of baseline case

4.1. Parameter preparation

The values of input decision variables (as listed in Table 3) are selected from a cellulosic biofuel production design reported by National Renewable Energy Laboratory (NREL) in USA [41] as the baseline case setup. Input feedstock is assumed as 1 kg for all following analysis. For the purpose of model calculation, the energy related parameters and chemical reaction parameters are listed in Table 4 and Table 5, respectively.

4.2. Energy consumption breakdown

In the baseline case, the total energy consumption is 2470.57 KJ, and the ethanol yield from 1 kg feedstock is 0.241 kg. The energy breakdown for each process is shown in Fig. 3. As can be seen from the figure, the pretreatment process contributes nearly half of the total energy consumption, although its residence time is much shorter compared to hydrolysis and fermentation. The main reason for such high energy consumption in the pretreatment process is the high-temperature reaction condition. Hence, it is expected that the development of energy-efficient pretreatment techniques will greatly benefit the sustainability of cellulosic biofuel production.

Fig. 4 illustrates the energy input to and output from the production system in each process. The values on right side of the y-axis are the energy supplied to the system, while the left side represents the energy released from the system. It is observed that the electric energy is provided to the grinding machines in the size reduction process. In pretreatment process, energy is supplied for heating and maintaining reaction temperatures; and the energy contained in heated steam and water is released for heat recovery. It should be noted that in enzymatic hydrolysis and fermentation processes, more energy is released by reactions than the energy input to balance the heat loss. Therefore, cooling energy is provided to these two processes to keep desired temperature levels. In practice, both hydrolysis and fermentation reactions are cooled by circling cooling water [56].

It is also observed in Fig. 4 that 275 KJ of energy is recovered in the pretreatment process, which can lead to more than 10% of total energy

Table 5
Reaction related parameters.

Arrhenius reaction rate parameters			
Reaction rate	A (1/s)		E_a (kJ/mol)
k_{xo}	1.0×10^{15} [54]		110.0 [54]
k_{xl}	8.0×10^{17} [54]		130.0 [54]
k_g	2.0×10^{22} [55]		180.0 [55]
k_{h2}	2.0×10^{7} [43]		5570 [43]
Molecular weights (g/mol) [41]			
M_x			132
M_{xo}			450
M_{xl}			150
M_g			162
M_{gl}			180
Inhibition constant (g/L) [52]			
K_g			0.1
K_{xl}			0.1
Other parameters			
ρ_w	1 kg/m^3	q_n	0.213 [28]
D_e	0.68×10^{-10} m^2/s [49]		
Overall substrate utilization rate (g/L) [53]			
$q_{emax,g}$			10.9
$q_{emax,x}$			3.27
$q_{smax,g}$			5.12
$q_{smax,x}$			1.59
Substrates inhibitory concentration (g/L) [53]			
$K_{i,x}$			186
$K_{i,g}$			600
$K_{i,x}$			186
$K_{i,x}$			600
Threshold ethanol concentration (g/L) [53]			
$P_{i,g}$			57.4
$P_{i,x}$			81.2
$P_{m,g}$			57.4
$P_{m,x}$			81.2

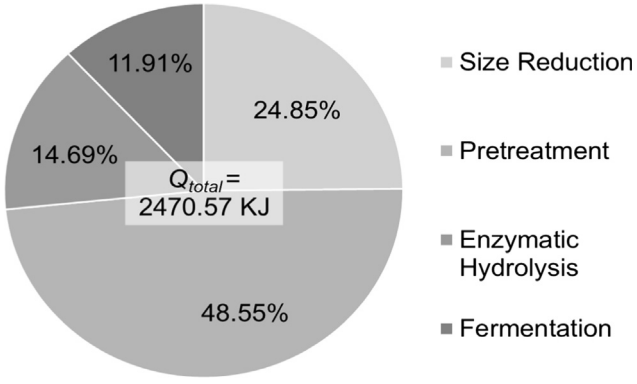

Fig. 3. Total energy consumption breakdown.

saving. In a commercial-scale biofuel production plant, energy efficiency could be significantly improved by adopting advanced heat recovery system. In addition, the energy consumed in the pretreatment process is 1474.4 KJ, 88% of which is contributed by heating.

The heating energy breakdown is shown in Fig. 5, where the energy for heating water and steam is accounted for more than 90%. Note that in this study, it is assumed that the biomass loading is a constant (1 kg), which makes the heating energy for biomass is unchanged. In addition, the specific heat capacity of water is much larger than biomass (reflected by Eqs. (3-1) and (3-2)), therefore, the water/biomass mass ratio becomes a main energy driver in this process. Further discussions on the impact of water/biomass ratio to the production system will be presented in Section 4.3.

4.3. Sensitivity analysis

In sensitivity analysis, nine decision variables are investigated as shown in Table 6. By adjusting the values of these nine decision variables, model calculation results (i.e., the total energy consumption and the final ethanol yield) are investigated as shown in Fig. 6.

According to the results shown in Figures, the following observations can be obtained.

(i) The total energy consumption and biofuel yield are positively correlated in most cases.
(ii) The water/biomass ratio has the most significant effect on the total energy consumption, and the pretreatment temperature is also an important factor. When water loading increases from 2 to 3 kg per kg feedstock, the production system consumes additional 25% energy, while the ethanol yield is decreasing. This indicates that a pretreatment reactor that can accommodate high solids loading will lead to the reduction of water usage and thus the energy consumed. However, in practice, high solid loading rate requires larger power of agitator and pumping machines, and sometimes is not necessarily pumpable.
(iii) Acid loading and fermentation time have the least impact on total energy consumption.
(iv) The ethanol yield reaches the maximum when the water/biomass ratio equals to 2, yet the yield is low when the ratio is at extreme values of its range. This can be explained as follows: if the initial water loading is high, the reaction rate will be low, which is reflected in Eqs. (7)—(10) of our model and can be further explained by the molecular collision theory; if initial water loading is low, the high concentration of the solution will lead to significant substrate/product inhibition, which is described analytically in Eqs. (9) and (10).
(v) In the case of feedstock size and pretreatment temperature, the total energy consumption shows non-monotonicity. The energy consumption reaches the maximum at feedstock size equals to 4 mesh. This might be because it consumes more energy to produce smaller feedstock particle size, which however, requires less energy in later biochemical conversions. Similarly, low pretreatment temperature will cause more energy consumption in the following processes and less energy recovery; however, high pretreatment temperature will cause substantial energy demand increase in the heating stage. Therefore, in Fig. 6(d), the lowest total energy consumption is achieved when the pretreatment temperature is at 166 °C.
(vi) Moreover, it is also observed that the effects of pretreatment time, enzymatic hydrolysis time, fermentation temperature and fermentation time on total energy consumed are near-linear, and the change of fermentation time has almost no impact on total energy consumption.

5. Energy consumption optimization using PSO

PSO is a metaheuristic technique for solving optimization problems, and it is originally proposed based on social–psychological principles to simulate the movement behavior of swarms such as bird flocks. Such swarms exhibit a property called swarm intelligence so that the complex behaviors of a big system can be accomplished efficiently by the combination of a group of subsystems (population) with simple individual behaviors [57].

In this paper, the energy consumption optimization problem is

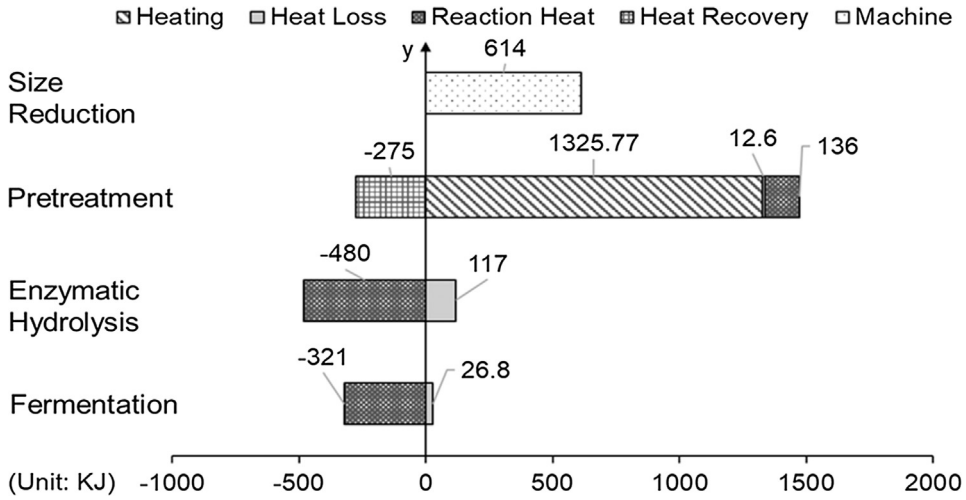

Fig. 4. Energy usage in each process from different sources.

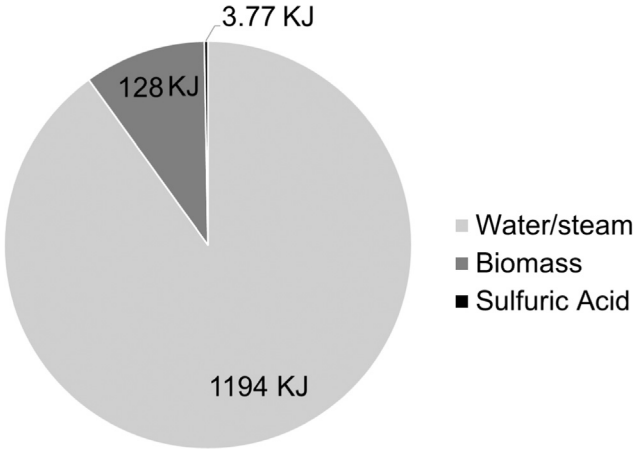

Fig. 5. Heating energy breakdown.

formulated as minimizing the total energy defined in Eq. (14) under the constraint of ethanol yield. The decision variables are selected to be the nine variables shown in Table 3. The nature of the biofuel production system energy consumption problem makes PSO an ideal approach because it is developed to solve problems with high complexity and non-linearity in high dimensional space.

5.1. Problem formulation

Let $\mathbf{S} = [L_2 \quad m_w \quad C_{acid} \quad T_p \quad t_p \quad T_h \quad t_h \quad T_f \quad t_f]$ be a potential solution that contains all the decision variables of the biofuel energy consumption problem. Based on the model developed in Eqs. (1)–(13), the optimization problem can be formulated as searching the variable values of **S** to minimize Q_{total} (Eq. (14)) while maintaining the desired ethanol yield. Let the final ethanol yield in baseline case (0.2411 kg ethanol/kg feedstock) be the minimum value for the optimization solution, then the problem can be formulated by Eqs. (14)–(24), where Eq. (14) represents the objective function; Eq. (15) shows the yield constraint; and Eqs. (16)–(24) define the feasible range of each decision variable.

$$\textit{Objective function}: \min (Q_{total}) \tag{14}$$

$$s.\ t. \quad ce_f \geqslant ce_{f,baseline} \tag{15}$$

$$2.54 \text{ mm} \leqslant L_2 \leqslant 25.4 \text{ mm} \tag{16}$$

$$1.5 \text{ kg} \leqslant m_w \leqslant 3 \text{ kg} \tag{17}$$

$$1\%\ w/w \leqslant C_{acid} \leqslant 3\%\ w/w \tag{18}$$

$$150\ ^\circ\text{C} \leqslant T_p \leqslant 170\ ^\circ\text{C} \tag{19}$$

$$4 \text{ mins} \leqslant t_p \leqslant 6 \text{ mins} \tag{20}$$

$$44\ ^\circ\text{C} \leqslant T_h \leqslant 52\ ^\circ\text{C} \tag{21}$$

$$72 \text{ hrs} \leqslant t_h \leqslant 96 \text{ hrs} \tag{22}$$

$$28\ ^\circ\text{C} \leqslant T_f \leqslant 36\ ^\circ\text{C} \tag{23}$$

$$28 \text{ hrs} \leqslant t_f \leqslant 36 \text{ hrs} \tag{24}$$

5.2. Solution procedure

In PSO, each possible solution is considered as a particle in the swarm. The population size (number of particles in the swarm) is denoted by N_p. Each particle is characterized by a position vector **X** and velocity vector **V**, so it can fly around the searching space over

Table 6
Data of the biofuel production energy sensitivity analysis.

Decision variables	Baseline setup	Range	Increment
Feedstock particle diameter: L_2	6.67 mm (4 mesh)	2.54–25.4 mm (1–10 mesh)	2.54 mm (1 mesh)
Water loading (per kg feedstock): m_w	2.2 kg	1.5–3 kg	0.15 kg
Diluted acid loading: C_{acid}	2.0% w/w	1–3% w/w	0.1% w/w
Pretreatment temperature: T_p	158 °C	150–170 °C	2 °C
Pretreatment time: t_p	5 min	4–6 min	0.2 min
Enzymatic hydrolysis temperature: T_h	48 °C	44 °C - 52 °C	1 °C
Enzymatic hydrolysis time: t_h	84 h	72–96 h	2 h
Fermentation temperature: T_f	32 °C	28–36 °C	1 °C
Fermentation time: t_f	36 h	30–42 h	1 h

iterations. A series of random numbers is generated for all decision variables in solution **S** from their ranges, and is used as the initial solution.

After initialization, the position and velocity are updated according to the optimality of the found solution:

$$\mathbf{V}_i(n+1) = \mathbf{V}_i(n) + c_1 w_1(\mathbf{S}_{PB,i}(n) - \mathbf{S}_i(n)) + c_2 w_2(\mathbf{S}_{GB}(n) - \mathbf{S}_i(n)), \quad i = (1, \ldots, N_p) \tag{25}$$

$$\mathbf{X}_i(n+1) = \mathbf{X}_i(n) + \mathbf{V}_i(n+1), \quad i = (1, \ldots, N_p) \tag{26}$$

where n and $n+1$ represent the n^{st} and $(n+1)^{st}$ iteration; c_1 and c_2 are learning factors; w_1 and w_2 are random numbers drawn from the unit uniform distribution Uniform (0,1); $\mathbf{S}_{PB,i}$ is the personal best solution (PBest) of the ith particle in n iterations; and $\mathbf{S}_{GB}$ represents the global best solution (GBest) of all particles in n iterations.

The fitness function of individual particles can be formulated by Eq. (27) with ethanol yield constraints (i.e., Eq. (15)) integrated as penalty terms, where M is a positive large real number. If the calculated ethanol yield is smaller than the baseline value, the fitness function will return a very large value so that the result will be rejected.

$$y = Q_{total} + M \cdot [\min(ce_f - ce_{f,baseline}, 0)]^2 \tag{27}$$

The learning factor c_1 and c_2 are set as 2; the maximum iteration number $N_{I,m}$ is set to be 100. The population size of 10, 20, 30, 50, 100 and 200 are tested to approach the near optimal solution. The algorithm terminates when the number of iteration reaches 100. The overall PSO algorithm is illustrated in Fig. 7.

5.3. Results analysis and discussion

The optimization results are obtained for population sizes of 10, 20, 30, 50, 100, and 200, where 20 trial runs are conducted for each size. The algorithm is coded in MATLAB and run by a desktop with 4 GB memory and 2.4 GHz Intel i5 CPU. The averaged time and statistical results to finish 100 iterations for the 6 population sizes (20 independent trial runs each) are provided in Table 7.

Fig. 8 shows the average values in 20 independent trail runs and 95% confidence interval of the optimized energy consumption for the 6

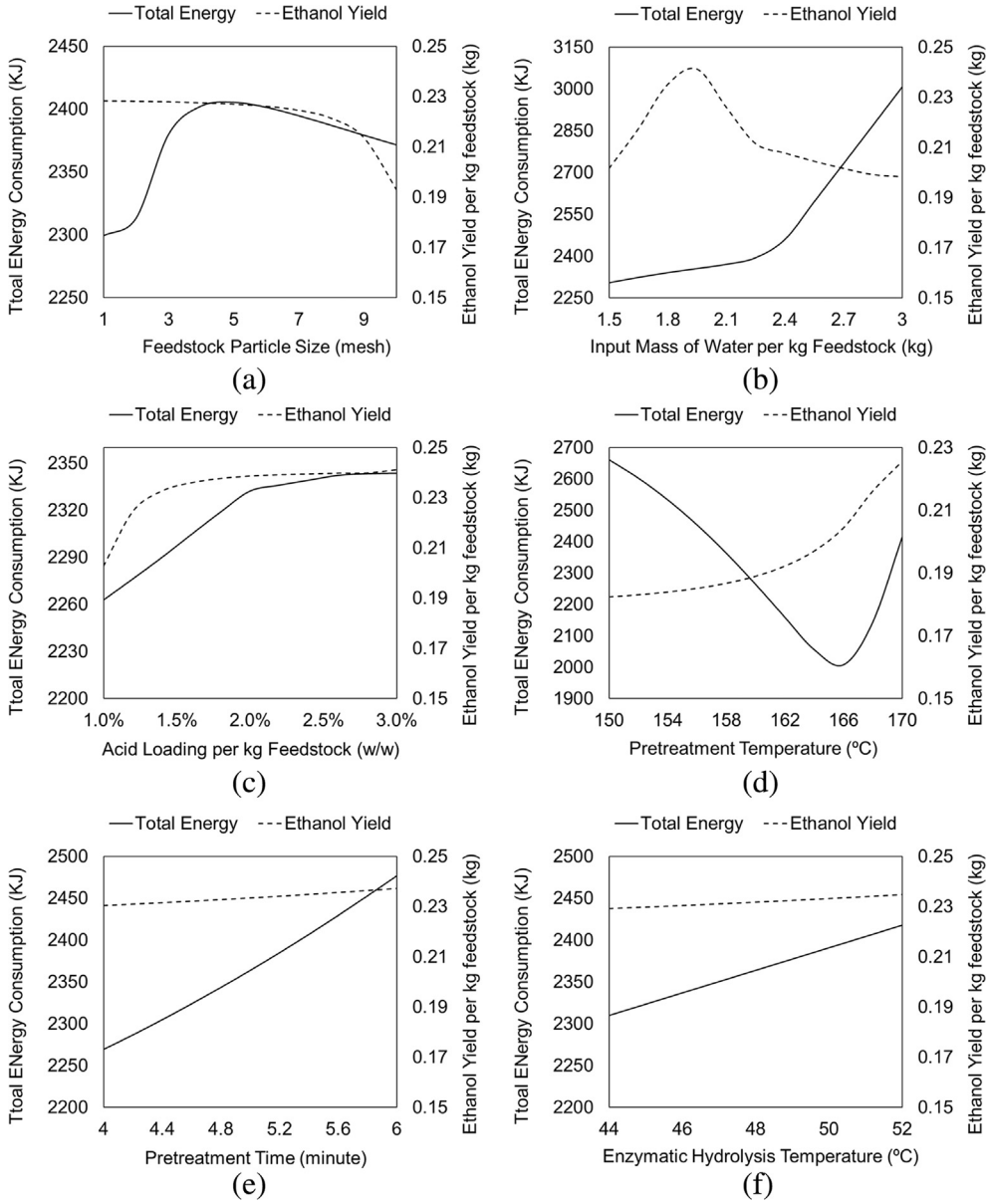

Fig. 6. Effects of (a) feedstock particle size, (b) water loading, (c) acid loading, (d) pretreatment temperature, (e) pretreatment time, (f) enzymatic hydrolysis temperature, (g) enzymatic hydrolysis time, (h) fermentation temperature and (i) fermentation time on total energy consumption and ethanol yield.

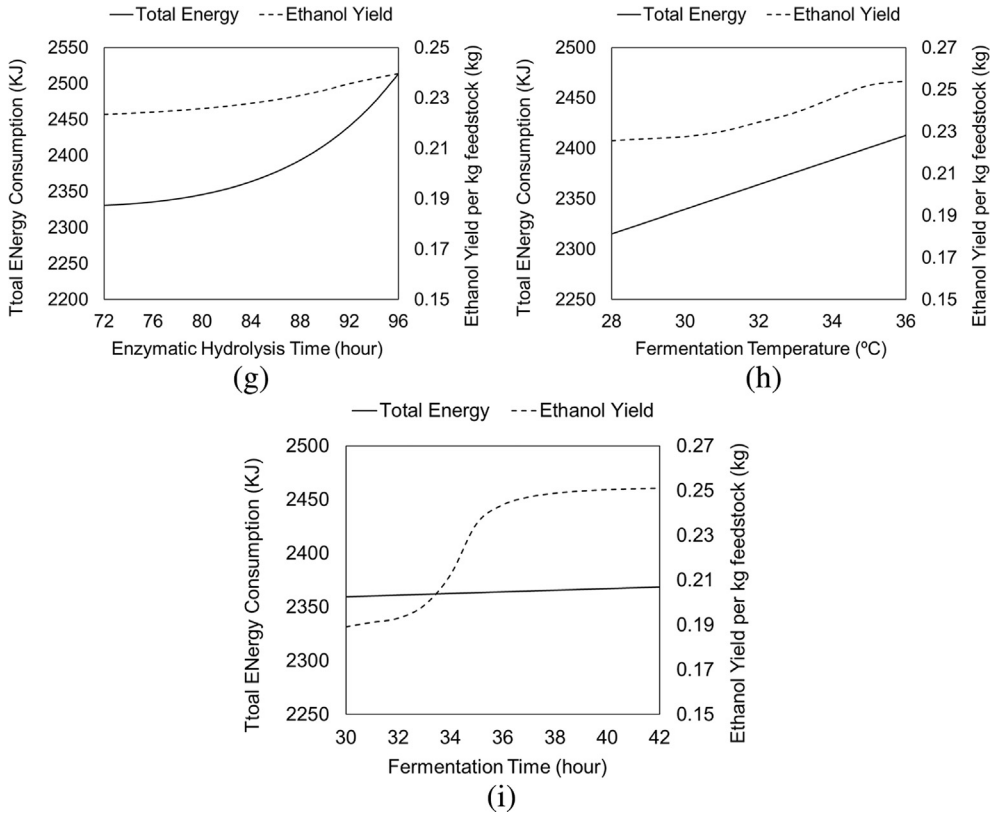

Fig. 6. (*continued*)

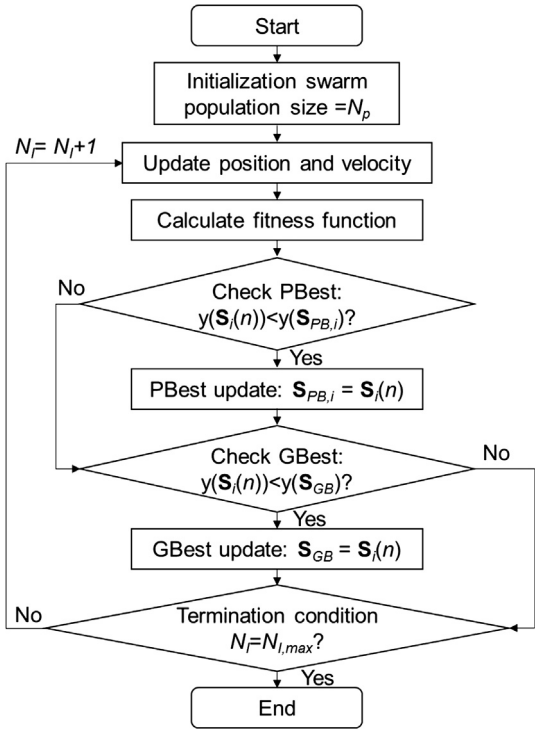

Fig. 7. Solution procedures of the energy optimization problem using PSO.

Table 7
The average time and statistical results of the energy consumption optimization problem in 6 different population sizes (20 trial runs for each size).

Population Size	Avg. time (second)	Min (KJ)	Mean (KJ)	Max (KJ)	Std. Dev.
10	0.2625	1964.3782	2101.1899	2242.9214	132.74
20	0.2944	1949.9644	1989.6188	2094.5133	54.9090
30	0.3418	1949.9644	1964.0309	1987.1477	13.3324
50	0.4268	1949.3492	1952.6224	1965.2769	4.7360
100	0.5814	1949.3472	1951.3232	1963.6914	4.4136
200	0.9316	1949.3468	1949.6940	1950.9635	0.5325

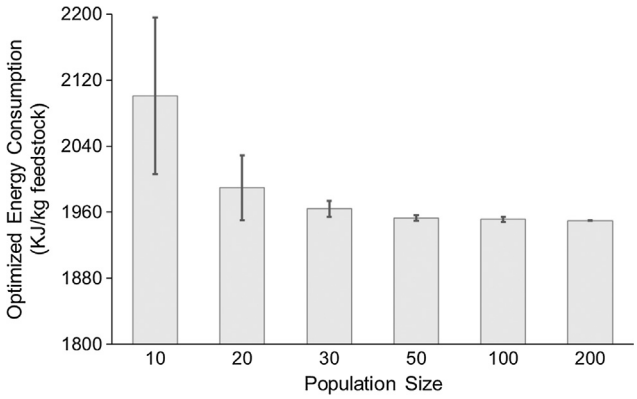

Fig. 8. Averaged optimal result of energy consumption with 95% confidence interval.

population sizes. When increasing the population size, the optimal value converges to around 1950 KJ/kg feedstock input, and the 95% confidence interval is also narrowed to (−0.38, 0.39). Therefore, we use the solution which results in the least total energy consumption among the 20 runs at population size of 200 as the near-optimal solution for the biofuel production energy consumption problem.

The results for the baseline case and solution obtained using the proposed optimization problem are shown in Table 8. Using solution obtained using the proposed optimization problem, 21.09% of the total

Table 8
Comparison of near-optimal solution and baseline case.

Decision variables	Baseline case	Near-optimal solution
Feedstock particle diameter: L_2	6.67 mm (4 mesh)	20.32 mm (8 mesh)
Water loading (per kg feedstock): m_w	2.2 kg	1.62 kg
Diluted acid loading: C_{acid}	1.0% w/w	2.49% w/w
Pretreatment temperature: T_p	158 °C	168.21 °C
Pretreatment time: t_p	5 min	4 min
Enzymatic hydrolysis temperature: T_h	48 °C	44 °C
Enzymatic hydrolysis time: t_h	84 h	93.68 h
Fermentation temperature: T_f	32 °C	28 °C
Fermentation time: t_f	36 h	42 h
Ethanol yield:	0.2411 kg/kg feedstock	0.2416 kg/kg feedstock
Total energy consumption:	2470.57 KJ/kg feedstock	1949.347 KJ/kg feedstock (21.09% reduction)

energy consumed by the biofuel production system is saved compared to the baseline case while maintaining ethanol yield.

6. Conclusions and future work

In this paper, an analytical system-level energy model for the cellulosic biofuel production system is established. This model comprehensively considers the interrelationships among multiple processes. Based on this model, the energy consumption for cellulosic biofuel production is optimized under the constraint of biofuel yield and solved using Particle Swarm Optimization (PSO) algorithm. In the proposed model, the fundamental relationships between the system energy consumption and production parameters are characterized, and the connection between energy and ethanol yield is established by mathematically modeling the chemical reactions. The case study results show that pretreatment is most energy-intensive of all processes in the cellulosic biofuel production system. The sensitivity analysis further indicates that the input water/biomass ratio has the most impact on the total energy consumption. Moreover, the near-optimal solution obtained from solving the optimization problem leads to 21.09% reduction in total energy consumption compared to the baseline case with no ethanol yield loss. The research outcomes will help realize energy-efficient biofuel production and enhance the sustainability of the cellulosic biofuel.

In the future, the model developed in this work can be further used to establish dynamic decision-making strategies for biofuel production systems, which can be used to monitor real-time production conditions and maintain the system energy consumption at a low level without loss in ethanol yield. This work can also be extended to study the overall energy consumption of biofuel from a supply chain perspective to further enhance the sustainability of the biofuel industry.

Acknowledgements

This work is supported by the U.S. National Science Foundation under Grant number 1434392.

References

[1] Jackson RB, Le Quéré C, Andrew RM, Canadell JG, Peters GP, Roy J, et al. Warning signs for stabilizing global CO_2 emissions. Environ Res Lett 2017;12:110202. http://dx.doi.org/10.1088/1748-9326/aa9662.
[2] Le Quéré C, Andrew RM, Friedlingstein P, Sitch S, Pongratz J, Manning AC, et al. Global carbon budget 2017. Earth Syst Sci Data Discuss 2017:1–79. http://dx.doi.org/10.5194/essd-2017-123.
[3] Amaro HM, Guedes AC, Malcata FX. Advances and perspectives in using microalgae to produce biodiesel. Appl Energy 2011;88:3402–10. http://dx.doi.org/10.1016/j.apenergy.2010.12.014.
[4] Hammond GP, Seth SM. Carbon and environmental footprinting of global biofuel production. Appl Energy 2013;112:547–59. http://dx.doi.org/10.1016/J.APENERGY.2013.01.009.
[5] Demirbas A. Political, economic and environmental impacts of biofuels: A review. Appl Energy 2009;86:S108–17. http://dx.doi.org/10.1016/J.APENERGY.2009.04.036.
[6] Lynd LR. The grand challenge of cellulosic biofuels. Nat Biotechnol 2017;35:912–5. http://dx.doi.org/10.1038/nbt.3976.
[7] Farrell AE, Plevin RJ, Turner BT, Jones AD, O'Hare M, Kammen DM. Ethanol can contribute to energy and environmental goals. Science (80-) 2006;311:506–8. http://dx.doi.org/10.1126/science.1121416.
[8] Huang HJ, Ramaswamy S, Al-Dajani W, Tschirner U, Cairncross RA. Effect of biomass species and plant size on cellulosic ethanol: A comparative process and economic analysis. Biomass Bioenergy 2009;33:234–46. http://dx.doi.org/10.1016/j.biombioe.2008.05.007.
[9] Pimentel D, Patzek TW. Ethanol production using corn, switchgrass, and wood; biodiesel production using soybean and sunflower. Nat Resour Res 2005;14:65–76. http://dx.doi.org/10.1007/s11053-005-4679-8.
[10] Vadas PA, Barnett KH, Undersander DJ. Economics and energy of ethanol production from alfalfa, corn, and switchgrass in the upper Midwest. USA. BioEnergy Res 2008;1:44–55. http://dx.doi.org/10.1007/s12155-008-9002-1.
[11] Sánchez ÓJ, Cardona CA. Trends in biotechnological production of fuel ethanol from different feedstocks. Bioresour Technol 2008;99:5270–95. http://dx.doi.org/10.1016/J.BIORTECH.2007.11.013.
[12] Cadoche L, López GD. Assessment of size reduction as a preliminary step in the production of ethanol from lignocellulosic wastes. Biol Wastes 1989;30:153–7. http://dx.doi.org/10.1016/0269-7483(89)90069-4.
[13] Miao Z, Grift TE, Hansen AC, Ting KC. Energy requirement for comminution of biomass in relation to particle physical properties. Ind Crops Prod 2011;33:504–13. http://dx.doi.org/10.1016/j.indcrop.2010.12.016.
[14] Vidal BC, Dien BS, Ting KC, Singh V. Influence of feedstock particle size on lignocellulose conversion – A review. Appl Biochem Biotechnol 2011;164:1405–21. http://dx.doi.org/10.1007/s12010-011-9221-3.
[15] Mani S, Tabil LG, Sokhansanj S. Grinding performance and physical properties of wheat and barley straws, corn stover and switchgrass. Biomass Bioenergy 2004;27:339–52. http://dx.doi.org/10.1016/j.biombioe.2004.03.007.
[16] Phanphanich M, Mani S. Impact of torrefaction on the grindability and fuel characteristics of forest biomass. Bioresour Technol 2011;102:1246–53. http://dx.doi.org/10.1016/j.biortech.2010.08.028.
[17] Yang B, Wyman CE. Pretreatment: the key to unlocking low-cost cellulosic ethanol. Biofuels, Bioprod Biorefining 2008;2:26–40. http://dx.doi.org/10.1002/bbb.49.
[18] Mesa L, Martínez Y, Barrio E, González E. Desirability function for optimization of Dilute Acid pretreatment of sugarcane straw for ethanol production and preliminary economic analysis based in three fermentation configurations. Appl Energy 2017;198:299–311. http://dx.doi.org/10.1016/J.APENERGY.2017.03.018.
[19] Maurya DP, Singla A, Negi S. An overview of key pretreatment processes for biological conversion of lignocellulosic biomass to bioethanol. 3. Biotech 2015;5:597–609. http://dx.doi.org/10.1007/s13205-015-0279-4.
[20] Yarbrough JM, Zhang R, Mittal A, Vander Wall T, Bomble YJ, Decker SR, et al. Multifunctional cellulolytic enzymes outperform processive fungal cellulases for coproduction of nanocellulose and biofuels. ACS Nano 2017;11:3101–9. http://dx.doi.org/10.1021/acsnano.7b00086.
[21] Liu G, Zhang J, Bao J. Cost evaluation of cellulase enzyme for industrial-scale cellulosic ethanol production based on rigorous Aspen Plus modeling. Bioprocess Biosyst Eng 2016;39:133–40. http://dx.doi.org/10.1007/s00449-015-1497-1.
[22] Zheng J, Tashiro Y, Wang Q, Sonomoto K. Recent advances to improve fermentative butanol production: Genetic engineering and fermentation technology. J Biosci Bioeng 2015;119:1–9. http://dx.doi.org/10.1016/J.JBIOSC.2014.05.023.
[23] Yu M, Zhang Y, Tang I-C, Yang S-T. Metabolic engineering of Clostridium tyrobutyricum for n-butanol production. Metab Eng 2011;13:373–82. http://dx.doi.org/10.1016/j.ymben.2011.04.002.
[24] Ou X, Zhang X, Chang S, Guo Q. Energy consumption and GHG emissions of six biofuel pathways by LCA in (the) People's Republic of China. Appl Energy 2009;86:S197–208. http://dx.doi.org/10.1016/J.APENERGY.2009.04.045.
[25] Kemppainen AJ, Shonnard DR. Comparative life-cycle assessments for biomass-to-ethanol production from different regional feedstocks. Biotechnol Prog 2008;21:1075–84. http://dx.doi.org/10.1021/bp049548q.
[26] Heyne S, Harvey S. Assessment of the energy and economic performance of second generation biofuel production processes using energy market scenarios. Appl Energy 2013;101:203–12. http://dx.doi.org/10.1016/j.apenergy.2012.03.034.
[27] Li L, Ge Y. System-level cost evaluation for economic viability of cellulosic biofuel manufacturing. Appl Energy 2017;203:711–22. http://dx.doi.org/10.1016/j.

apenergy.2017.06.074.
[28] Patzek TW. Thermodynamics of the corn-ethanol biofuel cycle, vol. 23, 2004. http://doi.org/10.1080/07352680490886905.
[29] Kesharwani R, Sun Z, Dagli C. Biofuel supply chain optimal design considering economic, environmental, and societal aspects towards sustainability. Int J Energy Res 2018;42:2169–98. http://dx.doi.org/10.1002/er.4006.
[30] Schmer MR, Vogel KP, Mitchell RB, Perrin RK. Net energy of cellulosic ethanol from switchgrass. Proc Natl Acad Sci 2008;105:464–9. http://dx.doi.org/10.1073/pnas.0704767105.
[31] Guinee JB. Handbook on life cycle assessment operational guide to the ISO standards. Int J Life Cycle Assess 2002;7:311–3. http://dx.doi.org/10.1007/BF02978897.
[32] Gonzalez-Salazar MA, Morini M, Pinelli M, Spina PR, Venturini M, Finkenrath M, et al. Methodology for estimating biomass energy potential and its application to Colombia. Appl Energy 2014;136:781–96. http://dx.doi.org/10.1016/j.apenergy.2014.07.004.
[33] Wang M, Wu M, Huo H. Life-cycle energy and greenhouse gas emission impacts of different corn ethanol plant types. Environ Res Lett 2007;2. http://dx.doi.org/10.1088/1748-9326/2/2/024001.
[34] Frankó B, Galbe M, Wallberg O. Bioethanol production from forestry residues: A comparative techno-economic analysis. Appl Energy 2016;184:727–36. http://dx.doi.org/10.1016/j.apenergy.2016.11.011.
[35] Tian S, Zhu W, Gleisner R, Pan XJ, Zhu JY. Comparisons of SPORL and dilute acid pretreatments for sugar and ethanol productions from aspen. Biotechnol Prog 2011;27:419–27. http://dx.doi.org/10.1002/btpr.545.
[36] Silva Ortiz P, de Oliveira S. Exergy analysis of pretreatment processes of bioethanol production based on sugarcane bagasse. Energy 2014;76:130–8. http://dx.doi.org/10.1016/j.energy.2014.04.090.
[37] Cardona Alzate CA, Sánchez Toro OJ. Energy consumption analysis of integrated flowsheets for production of fuel ethanol from lignocellulosic biomass. Energy 2006;31:2111–23. http://dx.doi.org/10.1016/j.energy.2005.10.020.
[38] Velásquez-Arredondo HI, Ruiz-Colorado AA, De Oliveira S. Ethanol production process from banana fruit and its lignocellulosic residues: Energy analysis. Energy 2010;35:3081–7. http://dx.doi.org/10.1016/j.energy.2010.03.052.
[39] Mafe OAT, Davies SM, Hancock J, Du C. Development of an estimation model for the evaluation of the energy requirement of dilute acid pretreatments of biomass. Biomass Bioenergy 2015;72:28–38. http://dx.doi.org/10.1016/j.biombioe.2014.11.024.
[40] Li L, Sun Z, Yao X, Wang D. Optimal production scheduling for energy efficiency improvement in biofuel feedstock preprocessing considering work-in-process particle separation. Energy 2016;96:474–81. http://dx.doi.org/10.1016/j.energy.2015.12.063.
[41] Humbird D, Davis R, Tao L, Kinchin C, Hsu D, Aden A, et al. Process design and economics for conversion of lignocellulosic biomass to ethanol. NREL Tech Rep NREL/TP-5100-51400, vol. 303, 2011. p. 275–3000.
[42] Sitaraman H, Kuhn EM, Nag A, Sprague MA, Tucker MP, Stickel JJ. Multiphysics modeling and simulation of high-solids dilute-acid pretreatment of corn stover in a steam-explosion reactor. Chem Eng J 2015;268:47–59. http://dx.doi.org/10.1016/j.cej.2015.01.020.
[43] Kadam KL, Rydholm EC, McMillan JD. Development and validation of a kinetic model for enzymatic saccharification of lignocellulosic biomass. Biotechnol Prog 2004;20:698–705. http://dx.doi.org/10.1021/bp034316x.
[44] Jeon YJ, Svenson CJ, Joachimsthal EL, Rogers PL. Kinetic analysis of ethanol production by an acetate-resistant strain of recombinant Zymomonas mobilis. Biotechnol Lett 2002;24:819–24. http://dx.doi.org/10.1023/A:1015546521000.
[45] Tanaka T. Comminution laws: Several Probabilities. Ind Eng Chem Process Des Dev 1966;5:353–8. http://dx.doi.org/10.1021/i260020a001.
[46] Austin LG, Klimpel RR. The theory of grinding operations. Ind Eng Chem 1964;56:18–29. http://dx.doi.org/10.1021/ie50659a004.
[47] Bitra VSP, Womac AR, Igathinathane C, Miu PI, Yang YT, Smith DR, et al. Direct measures of mechanical energy for knife mill size reduction of switchgrass, wheat straw, and corn stover. Bioresour Technol 2009;100:6578–85. http://dx.doi.org/10.1016/j.biortech.2009.07.069.
[48] Zheng Y, Pan Z, Zhang R. Overview of biomass pretreatment for cellulosic ethanol production. Int J Agric Biol Eng 2009;2:51–68. http://dx.doi.org/10.3965/j.issn.1934-6344.2009.03.051-068.
[49] Poling BE, Thomson GH, Friend DG, Rowley RL, Wilding WV. Perry's Chemical engineers' handbook, 2007. http://doi.org/10.1036/0071511253.
[50] Chemical statics and dynamics : Mellor, Joseph William, 1873-1938 : Free Download & Streaming : Internet Archive n.d. https://archive.org/details/chemicalstatics01mellgoog [accessed February 9, 2018].
[51] Crank J. The mathematics of diffusion. 2nd ed. UK: Oxford Univ Press; 1975. http://doi.org/10.1016/0306-4549(77)90072-X.
[52] Zhang YHP, Lynd LR. Toward an aggregated understanding of enzymatic hydrolysis of cellulose: Noncomplexed cellulase systems. Biotechnol Bioeng 2004;88:797–824. http://dx.doi.org/10.1002/bit.20282.
[53] Leksawasdi N, Joachimsthal EL, Rogers PL. Mathematical modelling of ethanol production from glucose/xylose mixtures by recombinant Zymomonas mobilis. Biotechnol Lett 2001;23:1087–93. http://dx.doi.org/10.1023/A:1010599530577.
[54] Esteghlalian A, Hashimoto AG, Fenske JJ, Penner MH. Modeling and optimization of the dilute-sulfuric-acid pretreatment of corn stover, poplar and switchgrass. Bioresour Technol 1997;59:129–36. http://dx.doi.org/10.1016/S0960-8524(97)81606-9.
[55] Wolfrum EJ, Sluiter AD. Improved multivariate calibration models for corn stover feedstock and dilute-acid pretreated corn stover. Cellulose 2009;16:567–76. http://dx.doi.org/10.1007/s10570-009-9320-2.
[56] Pretreatment D, Humbird D, Davis R, Tao L, Kinchin C, Hsu D, et al. Process design and economics for biochemical conversion of lignocellulosic biomass to ethanol. NREL Tech Rep NREL/LTP-5100-47764, vol. 147, n.d. http://doi.org/10.2172/1013269.
[57] Kennedy J, Eberhart RC, Shi Y. Swarm intelligence. Scholarpedia 2001;2:1462. http://dx.doi.org/10.4249/scholarpedia.1462.